

COBRA: A Continual Learning Approach to Vision-Brain Understanding

Xuan-Bac Nguyen¹, Arabinda Kumar Choudhary², Pawan Sinha³, Xin Li⁴, Khoa Luu¹

¹Department of Electrical Engineering and Computer Science, University of Arkansas, AR

²Department. of Radiology, SUNY Upstate Medical University, NY

³Department. of Brain & Cognitive Sciences, Massachusetts Institute of Technology, MA

⁴Department of Computer Science, SUNY Albany, NY

xnguyen@uark.edu, choudhaa@upstate.edu, psinha@mit.edu, xli48@albany.edu, khoaluu@uark.edu

Abstract

Vision-Brain Understanding (VBU) aims to extract visual information perceived by humans from brain activity recorded through functional Magnetic Resonance Imaging (fMRI). Despite notable advancements in recent years, existing studies in VBU continue to face the challenge of catastrophic forgetting, where models lose knowledge from prior subjects as they adapt to new ones. Addressing continual learning in this field is, therefore, essential. This paper introduces a novel framework called Continual Learning for Vision-Brain (COBRA) to address continual learning in VBU. Our approach includes three novel modules: a Subject Commonality (SC) module, a Prompt-based Subject Specific (PSS) module, and a transformer-based module for fMRI, denoted as MRIFormer module. The SC module captures shared vision-brain patterns across subjects, preserving this knowledge as the model encounters new subjects, thereby reducing the impact of catastrophic forgetting. On the other hand, the PSS module learns unique vision-brain patterns specific to each subject. Finally, the MRIFormer module contains a transformer encoder and decoder that learns the fMRI features for VBU from common and specific patterns. In a continual learning setup, COBRA is trained in new PSS and MRIFormer modules for new subjects, leaving the modules of previous subjects unaffected. As a result, COBRA effectively addresses catastrophic forgetting and achieves state-of-the-art performance in both continual learning and vision-brain reconstruction tasks, surpassing previous methods.

1. Introduction

Recently, vision-brain understanding (VBU) has made substantial progress due to advances in generative models, including GANs [53, 65] and Diffusion models [27, 55, 62, 63, 68, 72]. These approaches allow the reconstruc-

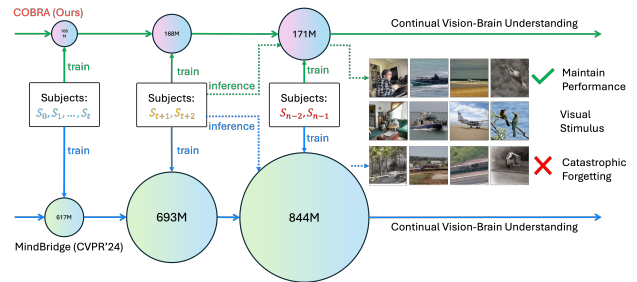


Figure 1. The paper introduces a novel framework, COBRA, for continual vision-brain understanding. In this figure, the sizes of the circles represent the network sizes. During the continual learning process, COBRA gradually increases the network sizes, while the previous method, MindBridge [72], expands the model sizes significantly. Furthermore, COBRA maintains performance, whereas MindBridge suffers from catastrophic forgetting. **Best viewed in color**

tion of increasingly realistic and accurate images from functional Magnetic Resonance Imaging (fMRI) signals. The approaches designed per-model-per-subject, as seen in [62, 68], are required to train a new model for a new subject. It can learn subject-specific but ignore subject-commonality features. To address this limitation, the studies [27, 55, 63, 72] proposed unified models trained on multiple subjects at a time. While these approaches are trained on a close set of subjects, they may still face a degradation in performance on new subjects. Recent efforts [63, 72] have aimed to adapt pre-trained models to new subject data, yet they continue to suffer from performance drops on prior subjects due to catastrophic forgetting [19, 59, 70], where models lose learned knowledge when adapting to new subject shifts. The ideal solution to this problem is to update the entire model with prior and new data. However, given the sensitive nature of brain data and the importance of privacy, retaining previous training data is often infeasible. Moreover, as the number of subjects grows, computational training costs become a concern. Thus, in practice, VBU models need to continually learn from new subjects without requir-

ing retraining on prior data. This paradigm is known as Continual Vision-Brain Understanding (CVBU). Given the limitation in previous brain understanding approaches, we raise critical questions for CVBU: (1) *What types of knowledge can the model retain*, and (2) *what types of knowledge must it learn specifically from new subject data?*

Since all subjects share similar patterns of brain activations [9, 13–17, 20, 22, 23, 74], if the model can understand these patterns, there is no need to learn from the data of new subjects. Consequently, the answer to the first question is to retain the knowledge of common patterns of brain activations learned from prior subjects and apply them to new ones. To achieve this, we propose a novel module designed to capture these patterns. Unlike prior methods [9, 13–17, 20, 22, 23, 74], our proposed approach can automatically identify a broader set of common patterns.

In addition to shared patterns of brain activations, each subject also has unique patterns. Therefore, in the continual brain understanding paradigm, the model must be able to adapt to these subject-specific patterns. This capability provides the answer to the second question. To achieve this, we draw inspiration from recent advancements in prompt-based learning or prompting [34]. This technique enables the model to receive learnable prompt tokens that flexibly incorporate additional task-specific information. In our approach, we treat subject-specific patterns as prompts representing unique information, which can then be learned and integrated from new subject data. This promises to mitigate the catastrophic forgetting problem in CVBU effectively.

Contributions of this Work: In summary, this work presents a novel continual learning approach to VBU. The contributions of this work can be summarized as follows. First, we introduce a new Continual Learning for Vision-Brain Understanding (COBRA) framework to the visual-brain understanding problem. To the best of our knowledge, this is the first work that tackles the vision-brain problem with a continual learning approach (detailed in Fig. 1). Second, a new Subject Commonality (SC) module will be presented to capture shared brain activation patterns across subjects. Unlike prior methods, COBRA can automatically identify a broader range of common patterns. Third, we present a new Prompt-based Subject-Specific (PSS) module to capture unique patterns specific to each subject. The module is trained to form the most relevant prompt, representing each subject’s distinct characteristics. Fourth, we introduce a novel MRIFormer module that contains a transformer encoder-decode to construct fMRI features for VBU. Apart from prior methods, this module can explore the sequence information, flexible and independent of any length of target features, i.e., Contrastive Language-Image Pre-Training (CLIP) features. Fifth, we introduce a simple yet effective training strategy to address the CVBU problem. In particular, COBRA is only required to update PSS and

Table 1. Summary of the advantages and limitations of the previous methods. *UM*: Unified model, *SCL*: Subject Commonality Learning, *SSL*: Subject Specific Learning, *CL*: Continual Learning

Method	UM	SCL	SSL	CL
Takagi [68]	✗	✗	✓	✗
MindEye1 [62]	✗	✗	✓	✗
Psychometry [63]	✓	✓	✓	✗
MindBridge [72]	✓	✓	-	✗
MindEye2 [63]	✓	✓	-	✗
NeuroPictor [27]	✓	✓	-	✗
UMBRAE [77]	✓	✓	-	✗
COBRA (Ours)	✓	✓	✓	✓

MRIFormer modules for new subjects. It leaves previous subjects’ PSS and MRIFormer unaffected, thus addressing catastrophic forgetting. Notably, the PSS module training is *label-free*, eliminating the need for additional annotations. The extensive experiments demonstrate our method achieves state-of-the-art (SOTA) performance in VBU and continual learning. The pros and cons of COBRA compared to prior methods are summarized in Table 1.

2. Related Work

2.1. Vision-Brain Understanding

In VBU, the fMRI signals corresponding to subjects’ viewing of an image are treated as input, which is then decoded to reconstruct the image originally viewed [27, 55, 62, 63, 68, 72, 77]. Many works have leveraged diffusion [11, 26, 60, 67, 78] to learn the fMRI signal distribution. MindEye [62] aligns the original image and fMRI latent spaces via contrastive learning and then uses diffusion to reconstruct the original image stimulus. MindEye2 [63] trains in a limited data setting to address expensive fMRI data acquisition. Takagi et al. [68] use latent diffusion [60] for image reconstruction, using a part of the fMRI as the diffusion conditioning. MindBridge [72] trains with a cyclic fMRI reconstruction mechanism, aligning brain data between subjects, allowing for more robust brain-to-image and text decoding using dual embeddings. Psychometry [55], by contrast, trains a singular model common and unique features for all subjects. NeuroPictor [27] uses a latent diffusion-like approach [60] to encode the fMRI signals into a latent space to separate high- and low-level features, giving the ability to focus on finer details. UMBRAE [77] decodes fMRI signals in a vision-language framework, aligning text descriptions and image features.

2.2. Continual Learning

We review two continual learning approaches [73], each with advantages and limitations. Rehearsal-based methods address catastrophic forgetting by storing sampled past tasks’ data in buffers [2, 4–7, 25, 54, 58, 66, 76], and thus in-

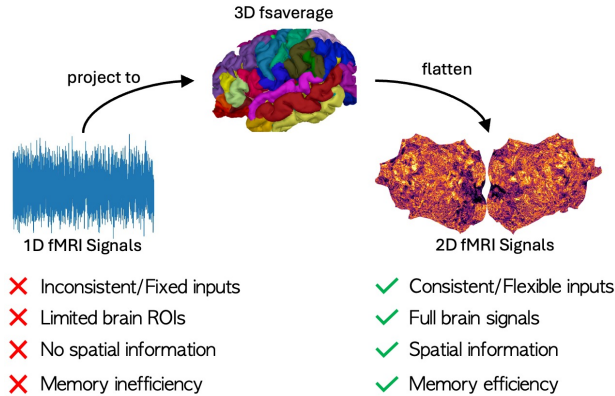


Figure 2. Limitations of previous work and our advancements in vision-brain representation.

tegrate old and new data to prevent knowledge loss. Several works leverage knowledge distillation to compress knowledge across older and newer tasks [2, 7, 58, 76] while others leverage self-supervised methods [4, 39–52, 54]. Key limitations include buffer size, where making too small degrade learning [4] and data privacy, restricting access to past data [66]. Architecture-based methods address catastrophic forgetting by modifying the architecture itself. Typically, this is done by adding a new set of parameters for new tasks [29, 35, 57, 61, 79, 81] or sub-networks specialized for a certain task are maintained [28, 37, 64, 75]. Key limitations include the added complexity of added parameters and the model needing the task type beforehand to select the task parameters, which is not guaranteed to be given at test time.

2.3. Limitations of Data Representation in Prior Methods

From prior studies, we have identified three main limitations, particularly concerning continual brain understanding and the unified model approaches.

L1. Since the brain sizes and structures of each subject differ, the sizes of fMRI signals vary across subjects. These signal sizes range from approximately 13,000 to 16,000 voxels per subject. Prior methods [3, 10, 24, 27, 31, 55, 62, 63, 68, 69, 72, 80] *fixed the input signal size* and adapted to new subjects with different input sizes. This poses a significant challenge to continual brain understanding, requiring methods to work with inputs with varying dimensions.

L2. Treating brain signals as one-dimensional (1D) vectors leads to a loss of spatial information. While voxels are closely connected to their neighbors in 3D space, flattening the signals into 1D disrupts these interactions. In particular, we observed that two samples in the signals may not be adjacent to each other spatially in 3D space, making it difficult to interpret the connections between them.

L3. Prior methods *rely on signals from specific Regions of Interest (ROI)*, such as floc-face, floc-body, and floc-place, rich in information about human visual perception. How-

ever, this focus may overlook other neighborhoods’ information. For instance, the floc-face area activates when a subject views a face in a visual stimulus, while the floc-body is responsible for human body perception. This approach might fail while facing with non-human subjects. To the best of our knowledge, no specific ROIs are dedicated to such common objects. Therefore, using signals from only the face, body, place, and word ROIs might miss critical information related to other elements in the visual stimulus.

3. The Proposed COBRA Approach

In this section, we first formulate the continual learning for vision-brain understanding in Section 3.1. Next, we present a data preprocessing approach as in Section 3.2 to address essential conditions so that our proposed modules, i.e., Subject Commonality (Section 3.3) and Prompt-based Subject Specific Modules (Section 3.4), can address introduced limitations **L1**, **L2**, **L3** as mentioned in Section 2.3.

3.1. Continual Vision-Brain Understanding

In this section, we first introduce continual brain understanding protocols. While typical CL is usually defined as training machine learning models on non-stationary data from sequential tasks, CVBU shares a similar idea. However, instead of increasing the tasks for the model as in CL, CVBU increases the number of subjects added to the most recent models.

We define a sequence of brain understanding tasks: $D = \{D_1 \dots D_S\}$, where the s^{th} subject $D_s = \{(v_i, x_i)\}_{i=1}^{n_s}$ is a set of pairs where each pair contains a visual stimulus $v_i \in \mathcal{V}$ and its corresponding record fMRI signals $x_i \in \mathcal{X}$. n_s is the number of samples for the task and i is the sample index of task dataset. The goal is to train a model $\mathcal{M}_\theta : \mathcal{X} \rightarrow \mathcal{V}$ to predict $v = \mathcal{M}_\theta(x) \in \mathcal{V}$ for any unseen sample from arbitrary subjects. In addition, the data of previous subjects are not available in the training process of new subjects.

3.2. Data Preprocessing

To address the limitations of **L1**, we adopt the 3D FreeSurfer [18] (fsaverage) space to represent the fMRI signals to the 2D forms. Since the 3D FreeSurfer is a general template of the human brain, it can effectively represent the fMRI signals of all subjects. In addition, the 3D FreeSurfer template offers 3D spatial information, which can help to address **L2**. While **L3** will be majorly addressed via our Subject Commonality Module (presented in the next section), we have found that the data preprocessing step plays an important role in providing the essential conditions to address **L3**. In particular, instead of using fMRI signals from specific ROIs, we use the entire brain signal, hypothesizing that the model will learn to identify the relevant regions for each ROI, automatically. In conclusion, representing brain signals in 2D addresses the previous limitations and offers

flexibility for various tasks like continual brain understanding and unified model learning. It provides an advanced approach to understanding the brain by leveraging CNNs or transformers. Fig. 2 (right-hand side) illustrates the representation of the 2D form of the fMRI signals. For convenience, in the rest of the paper, we refer to fMRI signals in the 2D flattened form instead of in 1D.

3.3. Subject Commonality Module

This section introduces the Subject Commonality (SC) module, designed to capture shared features across subjects. This module is inspired by neuroscience research to identify the functional localizers (floc) of brain patterns related to specific visual stimuli [9, 13–17, 20, 22, 23, 74]. This module also can address **L3** and discover ROIs of different categories rather than face, body, etc. Given the fMRI signals $x \in \mathbb{R}^{H \times W \times C}$ represented in 2D format, we define SC module as a transformer-based network, denoted as \mathcal{M}_c , to extract the commonality feature $f_c = [f_c^{\text{CLS}}, f_p] = \mathcal{M}_c(x) \in \mathbb{R}^{(L_c+1) \times D}$ where $f_p \in \mathbb{R}^{L_c \times D}$ contains high-level patch tokens which are output of Patch Embedding module, L_c is number of patches. $f_c^{\text{CLS}} \in \mathbb{R}^D$ denoted as CLS token. The goal of this module is to find out what objects fMRI signals are representing. The output of the SC module is formed as follows,

$$\begin{aligned} f_c &= [f_c^{\text{CLS}}, f_p] = \mathcal{M}_c(x) \in \mathbb{R}^{L_c \times D} \\ \hat{y}_c &= \text{MLP}_c(f_c^{\text{CLS}}) \in \mathbb{R}^{N_c} \end{aligned} \quad (1)$$

where MLP_c is a linear layer, \hat{y}_c is the predicted objects in the fMRI signals, N_c is number of object. In the Natural Scenes Dataset [1] (NSD), N_c is fixed to 80 since all stimuli are from the COCO [33] database. In addition, each stimulus contains multiple objects, for that reason, the $\mathcal{M}_c(x)$ is optimized using Binary Cross Entropy as in the Eqn (2).

$$\mathcal{L}_c = - \sum_{i=0}^{N_c-1} (y_{c,i} \times \log(\hat{y}_{c,i}) + (1 - y_{c,i}) \times \log(1 - \hat{y}_{c,i})) \quad (2)$$

Since \mathcal{M}_c is designed to receive the signal from any subjects, \mathcal{M}_c will learn *common* representation across subjects. Secondly, \mathcal{M}_c aims to learn the context inside the signals, i.e., what objects that signal contains.

3.4. Prompt-based Subject Specific (PSS) Module

Challenges. Let $x^{(a,v)}$ and $x^{(b,v)}$ denote the fMRI signals of a^{th} subject and b^{th} subject that are perceiving visual stimulus $v \in \mathcal{V}$. It is obvious that $x^{(a,v)} \neq x^{(b,v)}$ since they are collected from different persons. Since both subjects are seeing the same stimulus v , we can learn how different their brain patterns are by training a classification model \mathcal{M}_s to predict the signal $x^v \in \{x^{(a,v)}, x^{(b,v)}\}$ belonging to either subject a^{th} or b^{th} . In NSD, all subjects share 1,000 visual stimuli during recording. However, these samples belong to the testing set only, so we could not utilize them for training.

Motivations. Even if all subjects see different visual stimuli, they still experiment on the same set of objects $\mathcal{C} = \{\text{dog, cat, car, truck, \dots}\}$. Specifically, for the NSD database, \mathcal{C} is a set of 80 COCO classes. Instead of learning specific features across subjects on the same visual stimulus strictly, we learn subject-specific features via a similar context, i.e., f_c^{CLS} that subjects are viewing.

To achieve this goal, we draw inspiration from recent advances in prompt-based learning or prompting [34], a new transfer learning technique in natural language processing (NLP). Prompting techniques design model textual inputs with templated or learnable prompt tokens containing additional task-specific information. In this paper, we treat prompts as subject-specific features. We need to form a prompt that describes that unique.

Methods. First, we need to build a pool of prompt tokens where these tokens contain semantic information of fMRI signals. Fortunately, we found that the high-level tokens f_p can fulfill these requirements. Let $\mathcal{P} = \text{MLP}_p(f_p) \in \mathbb{R}^{L_c \times D}$ be prompt tokens where MLP_p is a linear layer. Let $\mathcal{K} \in \mathbb{R}^{L_c \times D}$ be a set of keys where each key will be associated with a token. To construct a prompt, we design the key-query paradigm to select the most k -suitable tokens w.r.t f_c^{CLS} as in the Eqn (3).

$$\begin{aligned} \text{sim} &= f_c^{\text{CLS}} \otimes \mathcal{K}^T \in \mathbb{R}^{L_c} \\ \text{index} &= \text{TopK}(\text{sim}, k) \\ f_s &= \text{IndexSelect}(\mathcal{P}, \text{index}) \in \mathbb{R}^{k \times D} \end{aligned} \quad (3)$$

where \otimes denotes a matrix multiplication operation, f_s is the subject-specific feature. We feed f_s into a pooling followed by a linear layer and then classify the feature corresponding to the right subjects as in Eqn (4).

$$\begin{aligned} \hat{y}_s &= \text{MLP}_s(\text{AvgPool}(f_s)) \in \mathbb{R}^{N_s} \\ \mathcal{L}_s &= - \sum_{i=0}^{N_s-1} y_{s,i} \times \log(\hat{y}_{s,i}) \end{aligned} \quad (4)$$

where N_s is the number of subjects. Interestingly, the training SSL module is *label-free* since all we need to know is the subject identity.

3.5. MRIFormer

With the subject common feature f_c from Eqn (1) and the subject-specific feature f_s from Eqn (3), we concatenate both to get the feature of fMRI signals as follows,

$$f = \text{concat}(f_c, f_s) \in \mathbb{R}^{(L_c+k) \times D} \quad (5)$$

The feature f contains multiple tokens from fMRI images and subject-specific prompts. We further feed f into a transformer encoder to accumulate information between commonalities and specific features as in Eqn (6).

$$f_h = \text{TransEnc}(f) \in \mathbb{R}^{(L_c+k) \times D} \quad (6)$$

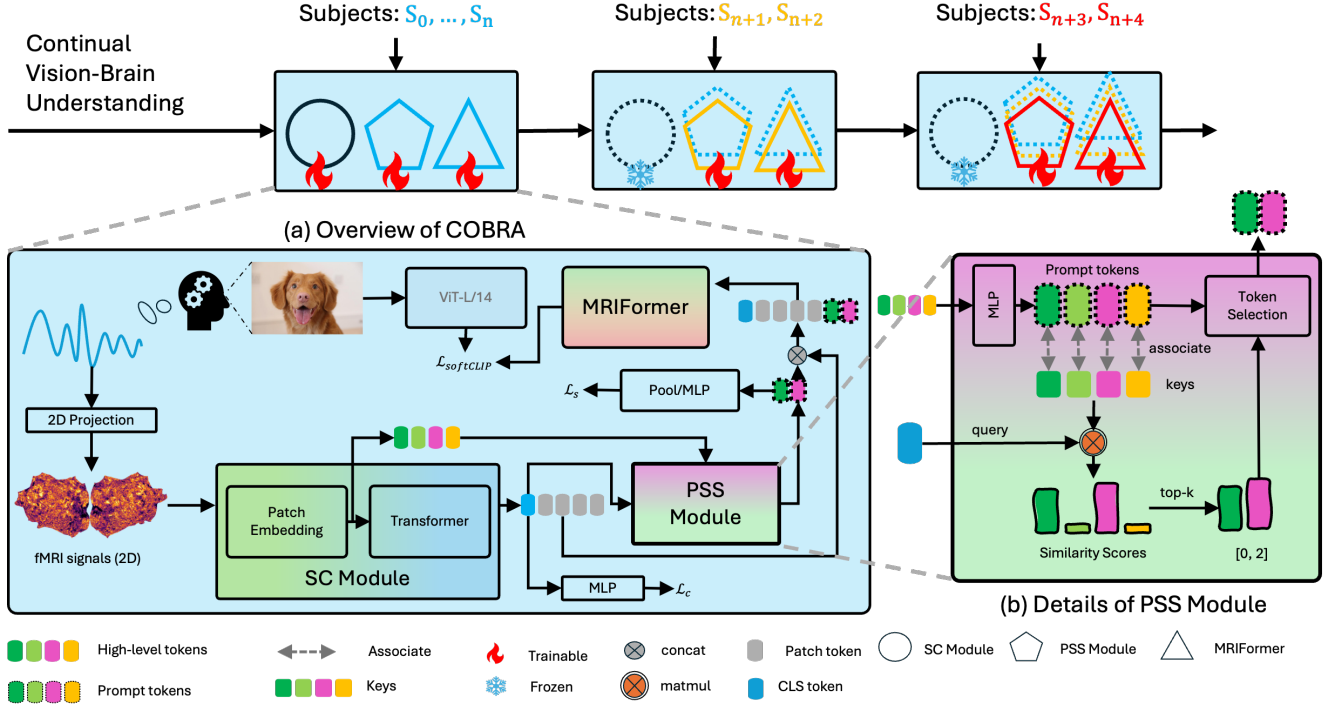


Figure 3. **Overview of the COBRA Framework.** COBRA comprises three modules: Subject Commonality (SC), Prompt-based Subject Specific (PSS), and MRIFormer. The SC module is designed to capture common vision-brain patterns across subjects, while the PSS module focuses on learning subject-specific patterns. The MRIFormer module is a transformer-based architecture, consisting of an encoder that integrates common and subject-specific features, and a decoder that transforms the fMRI feature into a unified CLIP space.

The feature f_h will be aligned with the corresponding Contrastive Language-Image Pre-Training (CLIP) feature of the visual stimulus: $f_{CLIP} = \mathcal{M}_{CLIP}(v) \in \mathbb{R}^{L_{CLIP} \times D}$. We observe an inconsistency in the length of the feature, i.e., $(L_c + k) \neq L_{CLIP}$. The prior studies [62, 63, 68, 72] used a linear layer to map the fMRI feature to the same length as the CLIP one. However, it will lose the sequence properties of a feature. To address this problem, we take inspiration from Neural Machine Translation to design a transformer decoder to *translate* fMRI features to CLIP features. This approach can preserve sequential information and address feature length inconsistency as in Eqn (7).

$$f_{mri} = \text{TransDecoder}(f_h, f_q) \in \mathbb{R}^{L_{CLIP} \times D} \quad (7)$$

where $f_q \in \mathbb{R}^{L_{CLIP} \times D}$ is a query vector. Finally, the f_{mri} feature is aligned with f_{CLIP} using Contrastive Loss [56] as in Eqn (8).

$$\mathcal{L}_{con} = -\frac{1}{N} \sum_i \left[\log \frac{\exp(\mathbf{p}_i \otimes \mathbf{q}_i / \sigma)}{\sum_j \exp(\mathbf{p}_i \otimes \mathbf{q}_j / \sigma)} - \log \frac{\exp(\mathbf{q}_i \otimes \mathbf{p}_i / \sigma)}{\sum_j \exp(\mathbf{q}_i \otimes \mathbf{p}_j / \sigma)} \right] \quad (8)$$

where $\mathbf{p} = f_{mri}$, $\mathbf{q} = f_{CLIP}$ and σ is the temperature.

3.6. Continual Training Strategy

As outlined in Section 3.1, CVBU involves updating models to accommodate new subject data without forgetting knowledge from previously trained subjects. Assuming the SC

module has acquired substantial knowledge from previous subjects, it focuses on learning subject-specific features of each new subject. Therefore, for each new subject added to the pipeline, we do not retrain or update the entire model. Instead, we only need to create new PSS and MRIFormer modules and train them to capture features specific to the new subject. Fig. 3 illustrates the pipeline of CVBU.

As in the CVBU, the size of MLP_s in Eqn (4) will be extended as the number of subjects increases. This layer holds *center vectors* of the subjects. Since we do not have access to previous subjects, the center vectors of previous subjects are not updated in the current steps of adapting new subjects. Therefore, the new center vector may be collapsed into the existing center vectors, making the PSS module fail to learn the specific feature. To address this problem, we add a regulation loss as follows,

$$\mathcal{L}_{reg} = \sum_{c_i, c_j} \{\max(0, 2\nabla - \|c_i - c_j\|)\}^2 \quad (9)$$

where c_i, c_j are the center vectors of i^{th} and j^{th} subjects and ∇ is the margin between centers.

Training Loss Functions. In summary, COBRA is trained using the objective loss function as follows,

$$\mathcal{L} = \lambda_c \mathcal{L}_c + \lambda_s \mathcal{L}_s + \lambda_{sc} \mathcal{L}_{con} + \lambda_{reg} \mathcal{L}_{reg} \quad (10)$$

where $\lambda_c, \lambda_s, \lambda_{sc}, \lambda_{reg}$ are the weights of the SC module,

Algorithm 1 Pseudo code for COBRA.

1: **Input:** The visual stimulus v , fMRI signals x
2: **Output:** The objective loss.
 ▷ *Commonality Module*
3: $f_c \leftarrow [f_c^{\text{CLS}}, f_p] \leftarrow \mathcal{M}_c(x)$
4: $\hat{y}_c \leftarrow \text{MLP}_c(f_c^{\text{CLS}})$
5: $\mathcal{L}_c \leftarrow -\sum_{i=0}^{N_c-1} (y_{c,i} \times \log(\hat{y}_{c,i}) + (1 - y_{c,i}) \times \log(1 - \hat{y}_{c,i}))$
 ▷ *Prompt-based Subject Specific Module*
6: $\mathcal{P} \leftarrow \text{MLP}_p(f_p)$
7: $\text{sim} \leftarrow f_c^{\text{CLS}} \otimes \mathcal{K}^T$
8: $\text{index} \leftarrow \text{TopK}(\text{sim}, k)$
9: $f_s \leftarrow \text{IndexSelect}(\mathcal{P}, \text{index})$
10: $\hat{y}_s \leftarrow \text{MLP}_s(\text{AvgPool}(f_s))$
11: $\mathcal{L}_s \leftarrow -\sum_{i=0}^{N_s-1} y_{s,i} \times \log(\hat{y}_{s,i})$
12: $\mathcal{L}_{reg} \leftarrow \sum_{c_i, c_j} \{\max(0, 2\nabla - \|c_i - c_j\|)\}^2$
 ▷ *MRIFormer*
13: $f \leftarrow \text{Concat}(f_c, f_s)$
14: $f_h \leftarrow \text{TransEnc}(f)$
15: $f_{mri} \leftarrow \text{TransDecoder}(f_h, f_q)$
16: $f_{CLIP} \leftarrow \mathcal{M}_{CLIP}(v)$
17: $\mathcal{L}_{con} \leftarrow \text{ContrastiveLoss}(f_{mri}, f_{CLIP})$
 ▷ *Training loss*
18: $\mathcal{L} \leftarrow \lambda_c \mathcal{L}_c + \lambda_s \mathcal{L}_s + \lambda_{sc} \mathcal{L}_{\text{softCLIP}} + \lambda_{reg} \mathcal{L}_{reg}$
19: **return** \mathcal{L}

PSS module, Soft CLIP, and regulation loss, respectively. The pseudo-code for COBRA is described in Algorithm 1.

3.7. Implementation Details

The 2D fMRI signals x are resized to 224×224 . We select `vit-base-16` as the SC module to extract patches’ feature of the fMRI signals. Each feature vector has dimension $D = 768$. In the PSS module, we design associated keys for prompt tokens as a vector of 197×768 . We select $k = 30$ as a top-k number. That means for each query of commonality feature f_c^{CLS} , we select top-30 tokens from the high-level tokens \mathcal{P} to describe specific features of the subject. The transformer encoder in Eqn (6) and the decoder in Eqn. (7) are designed to have four in-depth, dimension dim is 768, and the number of the head is set to 12. The framework is implemented via Pytorch and trained by $16 \times \text{A100 GPU}$ s (40GB each). The learning rate is set to $2.5e^{-5}$ initially and then reduced to zero gradually under CosineLinear [38] policy. The batch size is set to 32/GPU. The weight factors are set to one equally in the Eqn 10. The model is optimized by AdamW [36] for 300 epochs. The training is completed within two hours per subject, approximately.

4. Experimental Results

4.1. Dataset and Protocol

Dataset. Following common practices [3, 10, 24, 31, 69, 80], we utilize the Natural Scenes Dataset [1] for the brain understanding task. This dataset includes high-resolution 7-Tesla fMRI scans collected from eight healthy subjects who viewed thousands of natural images from MS-COCO [33].

Protocol. We propose two different CL scenarios. First, in

Table 2. Rehearsal-free continual learning results on NSD Testing Set. The bold numbers indicate the best results, while the underlines indicate the second-best results. The asterisk (*) indicates the results of our COBRA in cooperating with PLOP [12]. The dagger (\dagger) indicates the results of our COBRA trained on all subjects.

Method	(3,4)-(6,8)-(1,2)-(5,7) (4 steps)						(3,4,6,8)-(1,2,5,7) (2 steps)					
	(3,4,6,8)		(1,2,5,7)		all		(3,4,6,8)		(1,2,5,7)		all	
	SSIM	CLIP	SSIM	CLIP	SSIM	CLIP	SSIM	CLIP	SSIM	CLIP	SSIM	CLIP
W/o CL	0.197	58.9	0.216	60.6	0.207	59.8	0.197	59.7	0.238	61.1	0.218	60.4
LwF [30]	0.233	69.1	0.277	65.6	0.255	67.4	0.235	63.8	0.263	64.7	0.249	64.3
PLOP [12]	0.268	75.8	0.308	76.2	0.288	76.0	0.272	76.8	0.311	79.1	0.292	78.0
COBRA (Ours)	<u>0.311</u>	<u>93.2</u>	<u>0.344</u>	<u>93.1</u>	<u>0.328</u>	<u>93.2</u>	<u>0.316</u>	<u>92.3</u>	<u>0.342</u>	<u>93.4</u>	<u>0.329</u>	<u>92.9</u>
COBRA (Ours)*	0.325	94.4	0.351	94.8	0.338	94.2	0.322	93.5	0.345	93.8	0.333	93.7
COBRA (Ours) \dagger	0.336	96.9	0.365	97.2	0.351	97.1	0.336	96.9	0.365	97.2	0.351	97.1

the (3,4)-(6,8)-(1,2)-(5,7) setup, training begins with subjects (3,4), followed by subjects (6,8), (1,2), and (5,7) sequentially, for a total of four training steps. Second, in the (3,4,6,8)-(1,2,5,7) setup, the model is trained on subjects (3, 4, 6, 8) first, then (1, 2, 5, 7), for a total of two training steps. To evaluate the CL performance, we take the final model in each training scenario and test it on the test set of subjects (3,4,6,8) and (1,2,5,7). We also evaluate the performance of these models on all subjects.

Metrics. Similar to prior studies [3, 10, 24, 31, 69, 80], we adopt the Structural Similarity Index (SSIM) and Contrastive Language-Image Pre-Training (CLIP) score to evaluate the low-level and high-level reconstruction results.

4.2. Rehearsal-free Continual Learning

In this benchmark, we do not use any samples from the previous steps to train at the current step. The performance is presented in the Table 2. Without continual learning (W/o CL), performance drops significantly to 0.207 for the Structural Similarity Index (SSIM) and 59.8% for CLIP. Our COBRA approach achieves the scores of 0.320 for SSIM and 93.2% for CLIP, on average. It outperforms previous methods such as PLOP [12] and LwF [30] by 0.04 and 0.073 for SSIM, and 17.2% and 25.8% for CLIP, respectively. In the (3,4,6,8)-(1,2,5,7) setup, we observed similar results. COBRA achieves the scores of 0.329 for SSIM and 92.9 for CLIP, on average. It outperforms PLOP by 0.037 for SSIM and 14.8% for CLIP and LwF by 0.08 for SSIM and 28.6% for CLIP. Interestingly, we found that our COBRA can cooperate with the PLOP [12] method. By doing so, COBRA achieves higher performance, i.e., 0.01 for SSIM and 1% for CLIP in the 4-step scenario, and 0.004 for SSIM and 0.8% for CLIP in the 2-step scenario.

4.3. Rehearsal-based Continual Learning

In this learning setup, we evaluate performance when utilizing buffer data, i.e., 500, 1500, and 4000 samples per subject from previous subjects and jointly updating the model while training on new subjects. As shown in Table 3, performance improves gradually as the buffer size increases from 500 to 4000, approaching the upper bound. Compared to the previous rehearsal-based approach, C^o^2L [4], COBRA

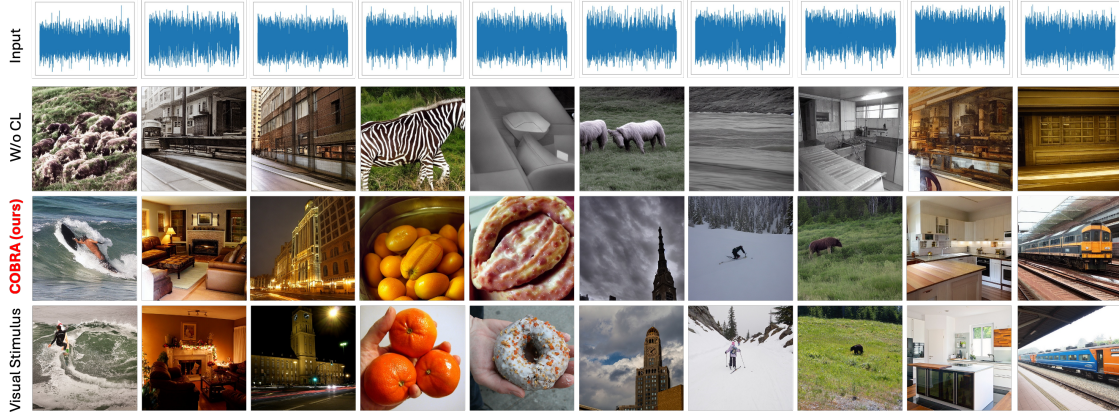


Figure 4. Qualitative results of the proposed COBRA in continual vision-brain understanding task. The first and top row is the input fMRI signals. The second row is the results without continual learning. The third row is the results of COBRA. The last row is the stimulus.

demonstrates superior continual learning performance, with average gains of 0.03, 0.042 in SSIM and 8.63%, 6.83% in CLIP across the 4-step and 2-step scenarios, respectively.

4.4. Qualitative Results

We demonstrate the vision-brain reconstruction results in the CL setups as in Fig. 4. COBRA maintains the high quality of the reconstructed results, while previous work does not. The context in the results of COBRA is clear and close to the visual stimulus. At the same time, without continual learning, one tends to generate a nonsensical sample due to the catastrophic forgetting problem.

Table 3. Rehearsal-based continual learning results on NSD test set for the vision-brain understanding task. The bold numbers indicate the best results.

Method	Buffer	(3,4)-(6,8)-(1,2)-(5,7) (4 steps)						(3,4,6,8)-(1,2,5,7) (2 steps)					
		(3,4,6,8)		(1,2,5,7)		all		(3,4,6,8)		(1,2,5,7)		all	
		SSIM	CLIP	SSIM	CLIP	SSIM	CLIP	SSIM	CLIP	SSIM	CLIP	SSIM	CLIP
Co^2L [4]	500	0.283	82.5	0.317	83.6	0.300	83.1	0.286	83.9	0.319	86.2	0.303	85.1
COBRA (Ours)		0.315	93.3	0.352	93.8	0.334	93.6	0.317	93.7	0.354	94.3	0.336	94.0
Co^2L [4]	1500	0.292	85.7	0.324	86.4	0.308	86.1	0.295	87.2	0.327	90.3	0.311	88.8
COBRA (Ours)		0.322	94.9	0.357	94.5	0.340	94.7	0.322	95.2	0.358	95.2	0.340	95.2
Co^2L [4]	4000	0.302	88.9	0.335	89.1	0.319	89.0	0.308	89.8	0.338	92.8	0.323	91.3
COBRA (Ours)		0.334	95.6	0.362	95.9	0.343	95.8	0.326	96.3	0.363	96.6	0.345	96.5

Table 4. Quantitative comparison of COBRA on reconstruction against other methods. We train COBRA on all subjects (no CL) of the NSD database. The bold number indicates the best result, while the underline indicates the second-best result.

Method	Low-Level				High-Level			
	PixCorr \uparrow	SSIM \uparrow	Alex(2) \uparrow	Alex(5) \uparrow	Incep \uparrow	CLIP \uparrow	Eff-B \downarrow	SwAV \downarrow
Mind-Reader [32]	-	-	-	-	66.5%	-	-	-
Mind-Vis [8]	0.67	0.196	67.7%	74.2%	67.9%	69.3%	0.898	0.513
Takagi [68]	-	-	74.0%	75.1%	67.3%	69.0%	-	-
Gu [21]	0.103	0.264	-	-	-	-	0.892	0.508
Psychometry [55]	<u>0.297</u>	0.340	<u>96.4%</u>	<u>98.6%</u>	95.8%	96.8%	0.628	0.345
MindBridge [72]	0.151	0.263	87.7%	95.5%	92.4%	94.7%	0.712	0.418
MindEye2 [63]	0.322	0.431	96.1%	<u>98.6%</u>	95.4%	93.0%	0.619	0.344
Neuropictor [27]	0.229	<u>0.375</u>	96.5%	98.4%	94.5%	93.3%	0.639	0.350
UMBRAE [77]	0.283	0.341	95.5%	97.0%	91.7%	93.5%	0.700	0.393
Ours (ViT-B)	0.243	0.351	92.1%	98.2%	<u>98.8%</u>	97.1%	0.619	0.336
Ours (ViT-H)	0.258	0.368	95.6%	<u>98.6%</u>	<u>98.8%</u>	<u>97.5%</u>	<u>0.602</u>	<u>0.321</u>
Ours (ViT-L)	0.284	<u>0.375</u>	96.5%	98.8%	98.9%	98.1%	0.593	0.318

4.5. Comparison To Previous SOTA Models Of Vision-Brain Reconstruction

In addition to our CL setup, we report the results of vision-brain reconstruction using various ViT models for the SC module. As in Table 4, with the SC module using ViT-L, we achieve the best scores on all metrics except PixCorr and SSIM (ranking second in SSIM). These findings highlight two major points. First, COBRA not only achieves SOTA results in the CL setup but is also competitive in general vision-brain reconstruction. Second, COBRA’s performance is responsible for the depth of the SC module, indicating the framework’s scalability. Fig. 5 shows superior reconstruction results compared to prior work.

4.6. Ablation Studies

Effectiveness of the vision-brain data representation. We compared COBRA’s performance when using full brain signals versus partial ROI signals as input, as shown in Table 5. Under identical settings, the model with full brain signals achieved 3% higher in SSIM and 2% higher in CLIP. It demonstrates that using full brain signals is significantly more effective than relying solely on partial ROI signals, as suggested by previous methods.

Effectiveness of the MRIFormer module. In COBRA, our MRIFormer includes a transformer encoder to accumulate subject-specific and individual information, and a transformer decoder to translate fMRI data into CLIP space. As shown in Table 5, compared to the linear layers used in prior studies, our module achieves approximately 3% higher performance in both SSIM and CLIP, which demonstrates the effectiveness of our approach.

Effectiveness of prompt length for PSS module. We evaluate the effectiveness of prompt length in the PSS module. In particular, we experiment with different top-k values as in the Eqn (3). The results are shown in Table 6. We found that selecting the top-k of 30 tokens for constructing the subject-specific prompt is the most optimal. Increasing this

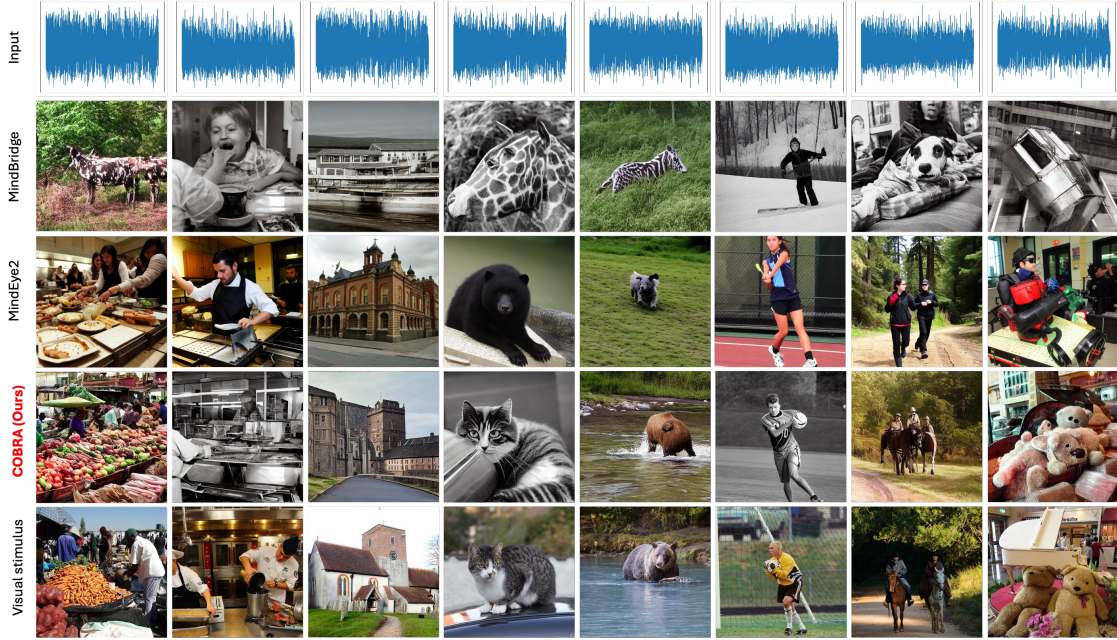


Figure 5. Qualitative comparison with the previous method on vision-brain reconstruction. The first row is the input fMRI signals. The next three rows are the results of MindBridge [72] and MindEye2 [63], and our COBRA. The last row is the stimulus.

top-k number does not improve overall performance, but increases network size.

Model sizes during continual learning. The size of COBRA grows gradually in response to an increasing number of subjects in CVBU. We simulate COBRA’s size as the number of subjects increases from 1 to 100. Additionally, we compare its model size to MindBridge[72] and MindEye2 [63], designed as a unified model. The results are shown in Fig. 6. Notably, the model size increases approximately nine times and three times for MindBridge and MindEye2 approximately as the subject count rises from 1 to 100. Meanwhile, COBRA’s size grows minimally. This is because only the PSS and MRIFormer modules expanded to additional subjects. Designed as lightweight and simple modules, the PSS and MRIFormer module adds relatively few parameters compared to MindBridge and MindEye2.

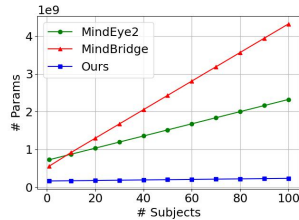


Figure 6. The size of model w.r.t number of subjects increasing.

Table 5. Ablation studies on using different input signals and effectiveness of MRIFormer. The bold numbers indicate the best results, while the underlines indicate the second-best results.

Input Data	fMRI Trans.	(3,4)-(6,8)-(1,2)-(5,7) (4 steps)				(3,4,6,8)-(1,2,5,7) (2 steps)			
		(3,4,6,8)		(1,2,5,7)		(3,4,6,8)		(1,2,5,7)	
		SSIM	CLIP	SSIM	CLIP	SSIM	CLIP	SSIM	CLIP
Partial ROI	Linear	0.263	85.9	0.265	86.2	0.264	86.1	0.276	86.4
Full Signals	Linear	0.288	88.2	0.291	89.4	0.290	88.8	0.293	88.9
Full Signals	MRIFormer	0.311	93.2	0.344	93.1	0.328	93.2	0.316	92.3

5. Conclusions

This work has presented one of the first continual learning approaches to the Vision-Brain Understanding problems. In particular, we have introduced the new Subject Commonality (SC) module to capture vision-brain patterns shared across subjects. In addition, the Prompt-based Subject-Specific (PSS) module has been designed to learn unique vision-brain patterns for each subject. The MRIFormer is also incorporated to align fMRI features with consistent CLIP features. In this continual learning setup, only the PSS module needs updating to accommodate new subjects, effectively addressing catastrophic forgetting. Our COBRA approach has achieved state-of-the-art performance in the VBU tasks, as demonstrated on the NSD benchmark.

Limitations and Future Work. Our SC module may be limited when the number of subjects is only one, as it does not effectively capture patterns shared across multiple subjects. The more subjects the module is trained on, the more accurately it can identify common patterns. In addition, this module is currently limited to 80 classes of MS-COCO. These limitations will motivate new research in future work.

Broader Impact. The advancements in deep learning and

Table 6. Ablation studies on different length of prompts. The bold numbers indicate the best results.

top-k	(3,4,6,8)-(1,2,5,7) (2 steps)					
	(3,4,6,8)		(1,2,5,7)		all	
	SSIM	CLIP	SSIM	CLIP	SSIM	CLIP
10	0.301	90.9	0.331	92.0	0.316	91.5
20	0.304	91.8	0.337	92.7	0.321	92.3
30	0.316	92.3	0.342	93.4	0.329	92.9
40	0.312	91.8	0.337	93.0	0.325	92.4

neuroscience hold transformative potential for adaptability in neuroscience applications. Implementing continual learning will empower researchers to identify common fMRI features based on a given condition in the future. This will facilitate more adaptable and sophisticated applications involving fMRI, such as the reconstruction of visual perception, decoding of internal speech, and development of neural prosthetics for communication.

References

- [1] Emily J Allen, Ghislain St-Yves, Yihan Wu, Jesse L Breedlove, Jacob S Prince, Logan T Dowdle, Matthias Nau, Brad Caron, Franco Pestilli, Ian Charest, et al. A massive 7t fmri dataset to bridge cognitive neuroscience and artificial intelligence. *Nature neuroscience*, 25(1):116–126, 2022. 4, 6
- [2] Pietro Buzzega, Matteo Boschini, Angelo Porrello, Davide Abati, and Simone Calderara. Dark experience for general continual learning: a strong, simple baseline, 2020. 2, 3
- [3] Mathilde Caron, Hugo Touvron, Ishan Misra, Hervé Jégou, Julien Mairal, Piotr Bojanowski, and Armand Joulin. Emerging properties in self-supervised vision transformers. In *Proceedings of the IEEE/CVF international conference on computer vision*, pages 9650–9660, 2021. 3, 6
- [4] Hyuntak Cha, Jaeho Lee, and Jinwoo Shin. Co2l: Contrastive continual learning. In *Proceedings of the IEEE/CVF International conference on computer vision*, pages 9516–9525, 2021. 2, 3, 6, 7
- [5] Arslan Chaudhry, Marc’Aurelio Ranzato, Marcus Rohrbach, and Mohamed Elhoseiny. Efficient lifelong learning with a-gem, 2019.
- [6] Arslan Chaudhry, Marcus Rohrbach, Mohamed Elhoseiny, Thalaiyasingam Ajanthan, Puneet K. Dokania, Philip H. S. Torr, and Marc’Aurelio Ranzato. On tiny episodic memories in continual learning, 2019.
- [7] Arslan Chaudhry, Albert Gordo, Puneet K. Dokania, Philip Torr, and David Lopez-Paz. Using hindsight to anchor past knowledge in continual learning, 2021. 2, 3
- [8] Zijiao Chen, Jiaxin Qing, Tiange Xiang, Wan Lin Yue, and Juan Helen Zhou. Seeing beyond the brain: Conditional diffusion model with sparse masked modeling for vision decoding, 2023. 7
- [9] Marcello Costantini, Cosimo Urgesi, Gaspare Galati, Gian Luca Romani, and Salvatore M Aglioti. Haptic perception and body representation in lateral and medial occipitotemporal cortices. *Neuropsychologia*, 49(5):821–829, 2011. 2, 4
- [10] Alexandre Défossez, Charlotte Caucheteux, Jérémy Rapin, Ori Kabeli, and Jean-Rémi King. Decoding speech perception from non-invasive brain recordings. *Nature Machine Intelligence*, 5(10):1097–1107, 2023. 3, 6
- [11] Prafulla Dhariwal and Alex Nichol. Diffusion models beat gans on image synthesis. *CoRR*, abs/2105.05233, 2021. 2
- [12] Arthur Douillard, Yifu Chen, Arnaud Dapogny, and Matthieu Cord. Plop: Learning without forgetting for continual semantic segmentation. In *Proceedings of the IEEE/CVF conference on computer vision and pattern recognition*, pages 4040–4050, 2021. 6, 1, 2
- [13] Paul E Downing, Yuhong Jiang, Miles Shuman, and Nancy Kanwisher. A cortical area selective for visual processing of the human body. *Science*, 293(5539):2470–2473, 2001. 2, 4
- [14] Brad Duchaine and Galit Yovel. A revised neural framework for face processing. *Annual review of vision science*, 1(1):393–416, 2015.
- [15] Russell Epstein and Nancy Kanwisher. A cortical representation of the local visual environment. *Nature*, 392(6676):598–601, 1998.
- [16] Russell Epstein, Alison Harris, Damian Stanley, and Nancy Kanwisher. The parahippocampal place area: recognition, navigation, or encoding? *Neuron*, 23(1):115–125, 1999.
- [17] Russell A Epstein and Chris I Baker. Scene perception in the human brain. *Annual review of vision science*, 5(1):373–397, 2019. 2, 4
- [18] Bruce Fischl, Martin I Sereno, Roger BH Tootell, and Anders M Dale. High-resolution intersubject averaging and a coordinate system for the cortical surface. *Human brain mapping*, 8(4):272–284, 1999. 3
- [19] Robert M French. Catastrophic forgetting in connectionist networks. *Trends in cognitive sciences*, 3(4):128–135, 1999. 1
- [20] Kalanit Grill-Spector, Kevin S Weiner, Kendrick Kay, and Jesse Gomez. The functional neuroanatomy of human face perception. *Annual review of vision science*, 3(1):167–196, 2017. 2, 4
- [21] Zijin Gu, Keith Jamison, Amy Kuceyeski, and Mert Sabuncu. Decoding natural image stimuli from fmri data with a surface-based convolutional network, 2023. 7
- [22] James V Haxby, Leslie G Ungerleider, Barry Horwitz, Stanley I Rapoport, and Cheryl L Grady. Hemispheric differences in neural systems for face working memory: A pet-rbf study. *Human Brain Mapping*, 3(2):68–82, 1995. 2, 4
- [23] James V Haxby, Leslie G Ungerleider, Barry Horwitz, Jose Ma Maisog, Stanley I Rapoport, and Cheryl L Grady. Face encoding and recognition in the human brain. *Proceedings of the National Academy of Sciences*, 93(2):922–927, 1996. 2, 4
- [24] James V Haxby, M Ida Gobbini, Maura L Furey, Alomit Ishai, Jennifer L Schouten, and Pietro Pietrini. Distributed and overlapping representations of faces and objects in ventral temporal cortex. *Science*, 293(5539):2425–2430, 2001. 3, 6
- [25] Tyler L. Hayes, Nathan D. Cahill, and Christopher Kanan. Memory efficient experience replay for streaming learning, 2019. 2
- [26] Jonathan Ho, Ajay Jain, and Pieter Abbeel. Denoising diffusion probabilistic models. *arXiv preprint arxiv:2006.11239*, 2020. 2
- [27] Jingyang Huo, Yikai Wang, Xuelin Qian, Yun Wang, Chong Li, Jianfeng Feng, and Yanwei Fu. Neuropictor: Refining fmri-to-image reconstruction via multi-individual pretraining and multi-level modulation. *arXiv preprint arXiv:2403.18211*, 2024. 1, 2, 3, 7

- [28] Zixuan Ke, Bing Liu, and Xingchang Huang. Continual learning of a mixed sequence of similar and dissimilar tasks, 2021. 3
- [29] Xilai Li, Yingbo Zhou, Tianfu Wu, Richard Socher, and Caiming Xiong. Learn to grow: A continual structure learning framework for overcoming catastrophic forgetting, 2019. 3
- [30] Zhizhong Li and Derek Hoiem. Learning without forgetting. *IEEE Transactions on Pattern Analysis and Machine Intelligence*, 40(12):2935–2947, 2018. 6, 1, 2
- [31] Victor Weixin Liang, Yuhui Zhang, Yongchan Kwon, Serena Yeung, and James Y Zou. Mind the gap: Understanding the modality gap in multi-modal contrastive representation learning. *Advances in Neural Information Processing Systems*, 35:17612–17625, 2022. 3, 6
- [32] Sikun Lin, Thomas Sprague, and Ambuj K Singh. Mind reader: Reconstructing complex images from brain activities, 2022. 7
- [33] Tsung-Yi Lin, Michael Maire, Serge Belongie, James Hays, Pietro Perona, Deva Ramanan, Piotr Dollár, and C Lawrence Zitnick. Microsoft coco: Common objects in context. In *Computer Vision—ECCV 2014: 13th European Conference, Zurich, Switzerland, September 6–12, 2014, Proceedings, Part V 13*, pages 740–755. Springer, 2014. 4, 6
- [34] Pengfei Liu, Weizhe Yuan, Jinlan Fu, Zhengbao Jiang, Hiroaki Hayashi, and Graham Neubig. Pre-train, prompt, and predict: A systematic survey of prompting methods in natural language processing. *ACM Computing Surveys*, 55(9): 1–35, 2023. 2, 4
- [35] Noel Loo, Siddharth Swaroop, and Richard E. Turner. Generalized variational continual learning, 2020. 3
- [36] I Loshchilov. Decoupled weight decay regularization. *arXiv preprint arXiv:1711.05101*, 2017. 6
- [37] Arun Mallya and Svetlana Lazebnik. Packnet: Adding multiple tasks to a single network by iterative pruning, 2018. 3
- [38] G Martino, Alberto Barrón-Cedeno, Henning Wachsmuth, Rostislav Petrov, and Preslav Nakov. Semeval-2020 task 11: Detection of propaganda techniques in news articles. *arXiv preprint arXiv:2009.02696*, 2020. 6
- [39] Hoang-Quan Nguyen, Xuan Bac Nguyen, Samuel Yen-Chi Chen, Hugh Churchill, Nicholas Borys, Samee U Khan, and Khoa Luu. Diffusion-inspired quantum noise mitigation in parameterized quantum circuits. *arXiv preprint arXiv:2406.00843*, 2024. 3
- [40] Hoang-Quan Nguyen, Thanh-Dat Truong, Xuan Bac Nguyen, Ashley Dowling, Xin Li, and Khoa Luu. Insect-foundation: A foundation model and large-scale 1m dataset for visual insect understanding. In *Proceedings of the IEEE/CVF Conference on Computer Vision and Pattern Recognition*, pages 21945–21955, 2024.
- [41] Pha Nguyen, Kha Gia Quach, Chi Nhan Duong, Ngan Le, Xuan-Bac Nguyen, and Khoa Luu. Multi-camera multiple 3d object tracking on the move for autonomous vehicles. In *Proceedings of the IEEE/CVF Conference on Computer Vision and Pattern Recognition*, pages 2569–2578, 2022.
- [42] Xuan-Bac Nguyen, Guee-Sang Lee, Soo-Hyung Kim, and Hyung-Jeong Yang. Audio-video based emotion recognition using minimum cost flow algorithm. In *2019 IEEE/CVF International Conference on Computer Vision Workshop (ICCVW)*, pages 3737–3741. IEEE, 2019.
- [43] Xuan-Bac Nguyen, Guee Sang Lee, Soo Hyung Kim, and Hyung Jeong Yang. Self-supervised learning based on spatial awareness for medical image analysis. *IEEE Access*, 8: 162973–162981, 2020.
- [44] Xuan-Bac Nguyen, Duc Toan Bui, Chi Nhan Duong, Tien D Bui, and Khoa Luu. Clusformer: A transformer based clustering approach to unsupervised large-scale face and visual landmark recognition. In *Proceedings of the IEEE/CVF conference on computer vision and pattern recognition*, pages 10847–10856, 2021.
- [45] Xuan Bac Nguyen, Apoorva Bisht, Hugh Churchill, and Khoa Luu. Two-dimensional quantum material identification via self-attention and soft-labeling in deep learning. *arXiv preprint arXiv:2205.15948*, 2022.
- [46] Xuan-Bac Nguyen, Chi Nhan Duong, Marios Savvides, Kaushik Roy, Hugh Churchill, and Khoa Luu. Fairness in visual clustering: A novel transformer clustering approach. *arXiv preprint arXiv:2304.07408*, 2023.
- [47] Xuan-Bac Nguyen, Xin Li, Samee U Khan, and Khoa Luu. Brainformer: Modeling mri brain functions to machine vision. *arXiv preprint arXiv:2312.00236*, 2023.
- [48] Xuan-Bac Nguyen, Xudong Liu, Xin Li, and Khoa Luu. The algonauts project 2023 challenge: Uark-ualbany team solution. *arXiv preprint arXiv:2308.00262*, 2023.
- [49] Xuan-Bac Nguyen, Hojin Jang, Xin Li, Samee U Khan, Pawan Sinha, and Khoa Luu. Bractive: A brain activation approach to human visual brain learning. *arXiv preprint arXiv:2405.18808*, 2024.
- [50] Xuan-Bac Nguyen, Hoang-Quan Nguyen, Samuel Yen-Chi Chen, Samee U Khan, Hugh Churchill, and Khoa Luu. Qclusformer: A quantum transformer-based framework for unsupervised visual clustering. *arXiv preprint arXiv:2405.19722*, 2024.
- [51] Xuan-Bac Nguyen, Hoang-Quan Nguyen, Hugh Churchill, Samee U Khan, and Khoa Luu. Hierarchical quantum control gates for functional mri understanding. *arXiv preprint arXiv:2408.03596*, 2024.
- [52] Bac Nguyen-Xuan and Guee-Sang Lee. Sketch recognition using lstm with attention mechanism and minimum cost flow algorithm. *International Journal of Contents*, 15(4):8–15, 2019. 3
- [53] Furkan Ozcelik, Bhavin Choksi, Milad Mozafari, Leila Reddy, and Rufin VanRullen. Reconstruction of perceived images from fmri patterns and semantic brain exploration using instance-conditioned gans. In *2022 International Joint Conference on Neural Networks (IJCNN)*, pages 1–8. IEEE, 2022. 1
- [54] Quang Pham, Chenghao Liu, and Steven Hoi. Dualnet: Continual learning, fast and slow, 2021. 2, 3
- [55] Ruijie Quan, Wenguan Wang, Zhibo Tian, Fan Ma, and Yi Yang. Psychometry: An omnifit model for image reconstruction from human brain activity. In *Proceedings of the IEEE/CVF Conference on Computer Vision and Pattern Recognition*, pages 233–243, 2024. 1, 2, 3, 7

- [56] Alec Radford, Jong Wook Kim, Chris Hallacy, Aditya Ramesh, Gabriel Goh, Sandhini Agarwal, Girish Sastry, Amanda Askell, Pamela Mishkin, Jack Clark, Gretchen Krueger, and Ilya Sutskever. Learning transferable visual models from natural language supervision, 2021. 5
- [57] Dushyant Rao, Francesco Visin, Andrei A. Rusu, Yee Whye Teh, Razvan Pascanu, and Raia Hadsell. Continual unsupervised representation learning, 2019. 3
- [58] Sylvestre-Alvise Rebuffi, Alexander Kolesnikov, Georg Sperl, and Christoph H. Lampert. icarl: Incremental classifier and representation learning, 2017. 2, 3
- [59] Anthony Robins. Catastrophic forgetting, rehearsal and pseudorehearsal. *Connection Science*, 7(2):123–146, 1995. 1
- [60] Robin Rombach, Andreas Blattmann, Dominik Lorenz, Patrick Esser, and Björn Ommer. High-resolution image synthesis with latent diffusion models, 2022. 2
- [61] Andrei A. Rusu, Neil C. Rabinowitz, Guillaume Desjardins, Hubert Soyer, James Kirkpatrick, Koray Kavukcuoglu, Razvan Pascanu, and Raia Hadsell. Progressive neural networks, 2022. 3
- [62] Paul Scotti, Atmadeep Banerjee, Jimmie Goode, Stepan Shabalín, Alex Nguyen, Aidan Dempster, Nathalie Verlinde, Elad Yundler, David Weisberg, Kenneth Norman, et al. Reconstructing the mind’s eye: fmri-to-image with contrastive learning and diffusion priors. *Advances in Neural Information Processing Systems*, 36, 2024. 1, 2, 3, 5
- [63] Paul S Scotti, Mihir Tripathy, Cesar Kadir Torrico Villanueva, Reese Kneeland, Tong Chen, Ashutosh Narang, Charan Santhirasegaran, Jonathan Xu, Thomas Naselaris, Kenneth A Norman, et al. Mindeye2: Shared-subject models enable fmri-to-image with 1 hour of data. *arXiv preprint arXiv:2403.11207*, 2024. 1, 2, 3, 5, 7, 8
- [64] Joan Serra, Dídac Surís, Marius Miron, and Alexandros Karatzoglou. Overcoming catastrophic forgetting with hard attention to the task, 2018. 3
- [65] Guohua Shen, Tomoyasu Horikawa, Kei Majima, and Yukiyasu Kamitani. Deep image reconstruction from human brain activity. *PLoS computational biology*, 15(1):e1006633, 2019. 1
- [66] Reza Shokri and Vitaly Shmatikov. Privacy-preserving deep learning. In *2015 53rd Annual Allerton Conference on Communication, Control, and Computing (Allerton)*, pages 909–910, 2015. 2, 3
- [67] Jascha Sohl-Dickstein, Eric A. Weiss, Niru Maheswaranathan, and Surya Ganguli. Deep unsupervised learning using nonequilibrium thermodynamics. *CoRR*, abs/1503.03585, 2015. 2
- [68] Yu Takagi and Shinji Nishimoto. High-resolution image reconstruction with latent diffusion models from human brain activity. In *Proceedings of the IEEE/CVF Conference on Computer Vision and Pattern Recognition*, pages 14453–14463, 2023. 1, 2, 3, 5, 7
- [69] Mingxing Tan. Efficientnet: Rethinking model scaling for convolutional neural networks. *arXiv preprint arXiv:1905.11946*, pages 6105–6114, 2019. 3, 6
- [70] Sebastian Thrun. Lifelong learning algorithms. In *Learning to learn*, pages 181–209. Springer, 1998. 1
- [71] Laurens Van der Maaten and Geoffrey Hinton. Visualizing data using t-sne. *Journal of machine learning research*, 9 (11), 2008. 1
- [72] Shizun Wang, Songhua Liu, Zhenxiong Tan, and Xinchao Wang. Mindbridge: A cross-subject brain decoding framework. In *Proceedings of the IEEE/CVF Conference on Computer Vision and Pattern Recognition*, pages 11333–11342, 2024. 1, 2, 3, 5, 7, 8
- [73] Zifeng Wang, Zizhao Zhang, Chen-Yu Lee, Han Zhang, Ruoxi Sun, Xiaoqi Ren, Guolong Su, Vincent Perot, Jennifer Dy, and Tomas Pfister. Learning to prompt for continual learning, 2022. 2
- [74] Kevin S Weiner, Michael A Barnett, Simon Lorenz, Julian Caspers, Anthony Stigliani, Katrin Amunts, Karl Zilles, Bruce Fischl, and Kalanit Grill-Spector. The cytoarchitecture of domain-specific regions in human high-level visual cortex. *Cerebral cortex*, 27(1):146–161, 2017. 2, 4
- [75] Mitchell Wortsman, Vivek Ramanujan, Rosanne Liu, Aniruddha Kembhavi, Mohammad Rastegari, Jason Yosinski, and Ali Farhadi. Supermasks in superposition, 2020. 3
- [76] Yue Wu, Yinpeng Chen, Lijuan Wang, Yuancheng Ye, Zicheng Liu, Yandong Guo, and Yun Fu. Large scale incremental learning, 2019. 2, 3
- [77] Weihao Xia, Raoul de Charette, Cengiz Öztireli, and Jing-Hao Xue. Umbrae: Unified multimodal brain decoding, 2024. 2, 7
- [78] Xingqian Xu, Zhangyang Wang, Eric Zhang, Kai Wang, and Humphrey Shi. Versatile diffusion: Text, images and variations all in one diffusion model, 2024. 2
- [79] Jaehong Yoon, Eunho Yang, Jeongtae Lee, and Sung Ju Hwang. Lifelong learning with dynamically expandable networks, 2018. 3
- [80] Hao Yu, Huanyu Wang, and Jianxin Wu. Mixup without hesitation. In *Image and Graphics: 11th International Conference, ICIG 2021, Haikou, China, August 6–8, 2021, Proceedings, Part II 11*, pages 143–154. Springer, 2021. 3, 6
- [81] Tingting Zhao, Zifeng Wang, Aria Masoomi, and Jennifer Dy. Deep bayesian unsupervised lifelong learning, 2021. 3

COBRA: A Continual Learning Approach to Vision-Brain Understanding

Supplementary Material

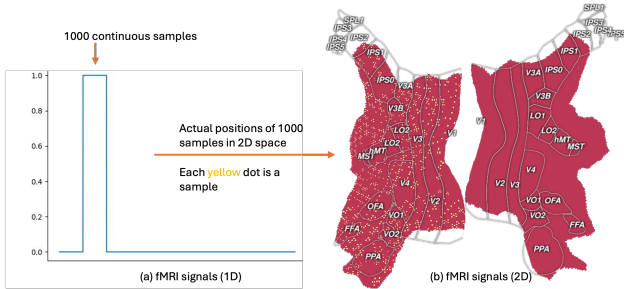


Figure 7. Demonstration of the spatial issue in 1D fMRI Signals.

6. Supplementary

6.1. Explanation of Spatial Issue in 1D fMRI Signals

In this section, We provide additional details about the spatial issue discussed in Section 3.2 regarding fMRI signals represented in 1D form. Specifically, for a given subject’s fMRI signals, we mask out all samples by setting their values to zero, retaining only *1000 continuous samples* and assigning their values to one. These modified signals are then projected onto the fsaverage surface for visualization, as shown in Fig. 7. It is evident that in the 1D form, the *1000 continuous samples* share strong correlations. However, when these signals are represented in 2D, the samples appear sparsely distributed. For that reason, analyzing fMRI signals in 1D form leads to a significant loss of spatial information.

6.2. Accuracy of SC and PSS Modules

In the proposed COBRA, the SC module is designed to remain fixed when training on new subjects, as it captures common vision-brain patterns learned from previous subjects. To verify this, we trained the SC module on subjects (3,4,6,8) and tested it on the unseen subjects (1,2,5,7). The SC module achieved an F1 score of 0.84, supporting our hypothesis. For the PSS module, we evaluated the PSS module’s accuracy in learning subject-specific features for each subject. It achieved a high accuracy of 98.5%, indicating that the module effectively selects prompts that represent subject-specific features. These results are presented in Table 7.

6.3. Visualization of Subject-Specific Features

In this section, we analyze the discrimination of subject-specific features, i.e., f_s , that is extracted from the PSS module. We employ T-SNE [71] to reduce the dimension of the features. The visualization is illustrated in Fig. 8. The

Table 7. Performance of SC and PSS module on their auxiliary tasks

Module	Metric	Accuracy
SC	f1 score	0.84
PSS	accuracy	98.5

result demonstrates that the PSS module was able to learn the specific features that are discriminative for the subjects.

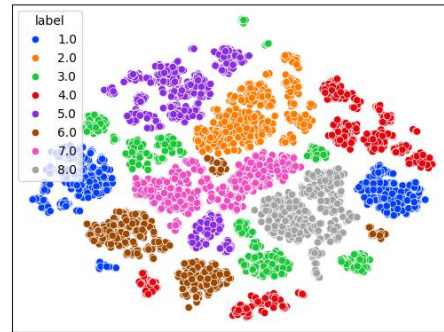


Figure 8. Visualization of the subject-specific features using T-SNE

6.4. Qualitative Comparison With Previous Continual Learning Approaches

In this section, we compare the qualitative vision-brain reconstruction results of the model under four scenarios: without any continual learning (CL) approach, using LwF [30], using PLOP [12], and our proposed method, COBRA. The results are illustrated in Fig. 9 and Fig. 10. Our proposed method demonstrates significantly better and clearer reconstruction results compared to previous methods. In contrast, LwF [30] and PLOP [12] lose critical contextual details. Notably, without applying any CL approach, the generated images are incoherent and fail to reconstruct the context meaningfully.



Figure 9. Qualitative comparison with the previous continual learning approaches on vision-brain reconstruction. From up to down, the first row is the results of not using the continual learning approach. The next two rows are the results of LwF [30] and PLOP [12], respectively. The last two rows are the results of COBRA and visual stimulus, correspondingly.

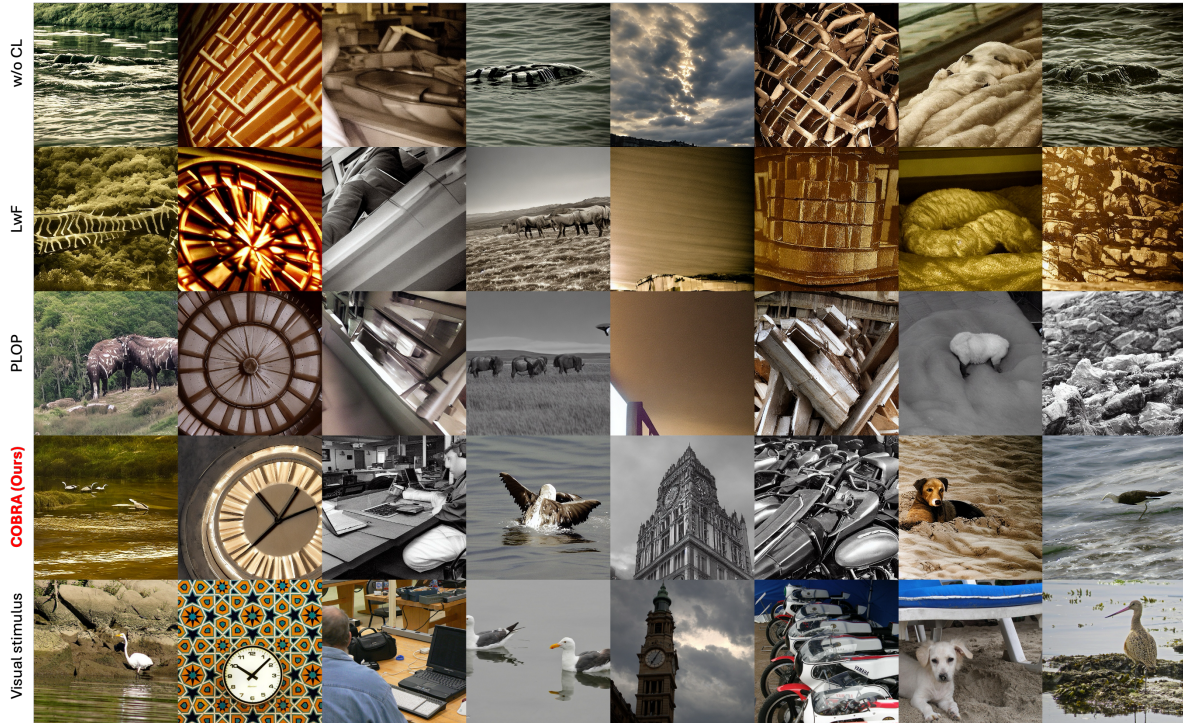


Figure 10. Qualitative comparison with the previous continual learning approaches on vision-brain reconstruction. From up to down, the first row is the results of not using the continual learning approach. The next two rows are the results of LwF [30] and PLOP [12], respectively. The last two rows are the results of COBRA and visual stimulus, correspondingly.